# Video Infringement Detection via Feature Disentanglement and Mutual Information Maximization

Zhenguang Liu
Zhejiang University
Hangzhou, Zhejiang, China
liuzhenguang2008@gmail.com

Xinyang Yu*
Zhejiang Gongshang University
Hangzhou, Zhejiang, China
xyyu2022@gmail.com

Ruili Wang
Massey University
Auckland, New Zealand
ruili.wang@massey.ac.nz

Shuai Ye
Zhejiang University
Hangzhou, Zhejiang, China
zzuyeh@163.com

Zhe Ma
Zhejiang University
Hangzhou, Zhejiang, China
mz.rs@zju.edu.cn

Jianfeng Dong*
Zhejiang Gongshang University
Hangzhou, Zhejiang, China
dongjf24@gmail.com

Sifeng He
Ant Group
Hangzhou, Zhejiang, China
hsf215kg@gmail.com

Feng Qian
Ant Group
Hangzhou, Zhejiang, China
youzhi.qf@antgroup.com

Xiaobo Zhang
Ant Group
Hangzhou, Zhejiang, China
ayou.zxb@antfin.com

Roger Zimmermann
National University of Singapore
Singapore, Singapore
rogerz@comp.nus.edu.sg

Lei Yang
Ant Group
Hangzhou, Zhejiang, China
yl149505@antgroup.com

## ABSTRACT

The self-media era provides us tremendous high quality videos. Unfortunately, frequent video copyright infringements are now seriously damaging the interests and enthusiasm of video creators. Identifying infringing videos is therefore a compelling task. Current state-of-the-art methods tend to simply feed high-dimensional mixed video features into deep neural networks and count on the networks to extract useful representations. Despite its simplicity, this paradigm heavily relies on the original entangled features and lacks constraints guaranteeing that useful task-relevant semantics are extracted from the features.

In this paper, we seek to tackle the above challenges from two aspects: (1) We propose to disentangle an original high-dimensional feature into multiple sub-features, explicitly disentangling the feature into exclusive lower-dimensional components. We expect the sub-features to encode non-overlapping semantics of the original feature and remove redundant information. (2) On top of the disentangled sub-features, we further learn an auxiliary feature to enhance the sub-features. We theoretically analyzed the mutual information between the label and the disentangled features, arriving at a loss that maximizes the extraction of task-relevant information from the original feature.

Extensive experiments on two large-scale benchmark datasets (*i.e.*, SVD and VCSL) demonstrate that our method achieves 90.1% TOP-100 mAP on the large-scale SVD dataset and also sets the new state-of-the-art on the VCSL benchmark dataset. Our code and model have been released at https://github.com/yyyooooo/DMI/, hoping to contribute to the community.

## CCS CONCEPTS

• **Computing methodologies** → **Visual content-based indexing and retrieval**.

## KEYWORDS

Video copyright infringements, neural network, mutual information

*Corresponding Authors

## 1 INTRODUCTION

Videos and images have become the most popular information source for us. A person may spend hours watching online videos, and an appealing video on YouTube could attract millions of views per day. The sheer number of videos on multiple internet platforms (such as Facebook and TikTok) has also brought along the issue of copyright infringement. Frequent video copyright infringements now turn into a major concern for *video creators* and *publishers*,

arXiv:2309.06877v1 [cs.CV] 13 Sep 2023

who have to spend numerous resources to prevent plagiarism and seek remedies for infringed works. As a result, infringing video retrieval has become an increasingly important task and has drawn intense attention from the research community.

Technically, a malicious user may directly copy a video and release it on another link or website. Such duplicate videos are trivial to be detected. However, malicious users usually conduct video editings to avoid infringement detection, the editings typically involve video cropping, blocking, flipping, splicing, *etc.* Fig. 1 demonstrates several video infringement examples.

Infringing video retrieval amounts to detecting similar and near-duplicate video pairs out from a video gallery. Over the past decade, *code books* [17] and *hashing functions* [32] have been popular solutions to generate video representations and enable video similarity computation. However, these models heavily depend on handcrafted features and shallow functions to identify infringements, leading to unsatisfactory performance. Recently, deep learning models [7, 39, 40, 42] have become the dominant approaches in infringing video retrieval, by virtue of their capacity to learn non-linear functions and sophisticated feature representations. One line of work attempts to fuse all the frame features into a single video-level representation and perform similarity matching on such representations [21, 23, 24]. Another line of work computes a frame-to-frame similarity matrix for all the frame-level features, and subsequently combines the matrix elements into a video-level similarity score [1, 15, 34].

Fundamentally, given an input video pair, the essence of infringing video retrieval is to obtain their feature representations, which capture their content similarity and disregard the superficial differences (such as *varying video encodings, noises* or *pixel-level differences*). Upon investigating and experimenting on the released implementations of state-of-the-art approaches [14, 21, 23], we empirically observe that two issues still persist: **(1)** Although existing methods have shown promising results in retrieving near-duplicate video pairs, they still have difficulties in identifying complicated cases where two videos are not explicitly similar, *e.g.*, *an infringing video might be obtained by cutting out part of the frame, video splicing, or blocking part of the frames.* **(2)** Current state-of-the-art methods rely on neural networks to extract label-relevant (in this task the label indicates whether two videos are similar) representations from the original feature, lacking mathematical constraints guaranteeing that useful cues are extracted and redundant information is reduced. Consequently, the final video embedding may overfit to trivial features or insufficient representations, which compromises the performance and robustness of such methods.

In this paper, we believe it would be fruitful to investigate whether introducing supervision to disentangle the features and enforce task-relevant feature extraction would facilitate the task. With this goal in mind, we come up with the following designs. (i) Following the theoretical analysis steeped in the framework of contrastive learning and Kullback–Leibler divergence, we explicitly disentangle the original feature into a group of non-overlapping sub-features. (ii) On top of the sub-features, we further engage in mutual information theory to extract an auxiliary feature from the original feature. The sub-features and the auxiliary feature together are composed into the final global feature. We attempt to maximize the mutual information between the label and the auxiliary feature so that no

task relevant information is dropped. This framework follows a maximum relevancy and minimum redundancy paradigm, serving to remove superfluous information and retaining as much useful information as possible for the end task.

We extensively evaluate the proposed method on two large-scale benchmark datasets (*i.e.*, SVD and VCSL). Empirical evaluations show that our approach significantly outperforms current state-of-the-art methods. Specifically, our method achieves 90.1% TOP-100 mAP on the large SVD dataset and also sets the new state-of-the-art performance on the VCSL benchmark dataset. Our code has been submitted to Github and are availabel at https://github.com/yyyooooo/DMI/ . We also present extensive ablation analyses on the contribution of each component, and evaluate the efficacy of feature disentangling and the proposed mutual information loss.

To summarize, our contributions are:

- We introduce a novel framework for extracting disentangled sub-features, which incorporates KL divergence maximization and contrastive learning to supervise the sub-feature learning process. The disentangled sub-features each serves to preserve an unique aspect of the original feature and is closely-related to the end task.
- In order to further extract task relevant information missed by the sub-features, we propose an auxiliary feature extraction method entrenched in the mutual information theory, which seeks to distill as much task relevant information from the original feature as possible.
- Extensive experiments on the large-scale SVD and VCSL benchmark datasets show that our method surpasses state-of-the-art approaches. Interesting findings and insights on feature disentanglement, original feature selection, and existing methods are presented.

## 2 RELATED WORK

In this section, we provide a brief holistic overview on the literature that is closely pertinent to this work. Roughly, the closely-related literature can be cast into 3 categories, namely *video retrieval, contrastive learning*, and *mutual information theory*.

### 2.1 Video Retrieval

Earlier approaches for video retrieval mainly revolve around code books [2, 20, 22] and hashing functions [32, 33] for encoding a video into a low-dimensional representation. Fueled by the success of deep learning [6, 10, 25, 27, 28, 41] in recent years, the predominant approaches are to decompose the video into frames and feed them into an image extraction backbone network, obtaining a sequence of image feature representations. One approach is to fuse all these image features into a single video-level representation and perform similar video pair detection on video-level representations [21, 23, 24]. Another approach is to compute a frame-to-frame similarity matrix for all the frame-level features, and subsequently combine the matrix elements into a video-level similarity score [1, 15, 34]. However, current methods heavily rely on the network architecture to extract effective representations from the input video pair, with no explicit mathematical constraints that can be leveraged to enforce extraction of useful semantic cues and removal of redundancies. Our work seeks to address this research gap by proposing a new

**Figure 1: Video infringement usually involves video editings such as video cropping, blocking, flipping, splicing, etc. The left most column shows the original video and the right columns show the modified videos.**

knowledge distillation framework tailored for the video retrieval task.

## 2.2 Contrastive Learning

Contrastive learning, which is typically done in a self-supervised manner, seeks to learn a representation that forces dissimilar videos to be far away from each other in the encoding space and similar videos to be close to each other [5, 11]. One seminal work [30] proposes the InfoNCE loss as an effective contrastive learning objective. Furthermore, [4] presents SimCLR, which engageed in data augmentations to generate positive (similar) pairs. Another landmark work, MoCo [11], improves upon the InfoNCE work through the use of a momentum contrast mechanism that improves convergence. [43] further advocates to train convolutional neural networks with contrastive learning and hard data augmentation, trying to explore more discriminative representations. Both [5] and [43] employ a similar strategy of data augmentation and take an augmented image as a positive (similar) sample. Such data augmentations include *cropping, grayscale, blocking part of the picture*, and *horizontal flipping*, which are quite similar to the strategies adopted in video infringement.

## 2.3 Mutual Information Theory

The mutual information of two random variables gives a quantitative measurement of the mutual dependency between them. The seminal work [36, 37] of information bottleneck theory present mathematical backgrounds of statistical learning and deep learning in the framework of mutual information. The theory put forth by the authors plays an indispensable role for carrying out information distillation by eliminating irrelevant input noises and preserving only those that are necessary for the task at hand. Estimating mutual information of two variables from their unknown distributions is notoriously challenging by nature. Recent works, such as [26, 35, 44],

propose a variational self-distillation approach to estimate mutual information, which can be combined effectively with backpropagation training in the deep learning life-cycle. Inspired by this, we embrace mutual information to perform feature level supervision that constrains label-relevant representation distillation.

## 3 METHOD

**Problem** Presented with a query video $q$ and a video gallery $\{g_i\}_{i=1}^n$, we are interested in retrieving all similar videos of $q$ from the video gallery. Specifically, we seek to learn an embedding for each video, where the similarity of a video pair can be conveniently computed via the distance between their respective embedding vectors. In other words, our task can be deemed as a supervised metric learning problem where the effectiveness of the embedding is assessed based on whether similar videos have a correspondingly smaller distance in the embedding space. Unsurprisingly, the embedding vectors for dissimilar videos should be far apart and have a low similarity score.

## 3.1 Method Overview

Broadly, we outline the proposed framework in Figure 2. First, we employ a pre-trained backbone network, such as MoCoV3 [11] and VGG [31], to extract a sequence of frame-level features from each input video. Subsequently, we fuse all frame-level features through average pooling, to get a video-level original feature for each video.

Given the original feature $V$ for a video, **(1)** we propose a subfeatures extraction module, which extracts a total of $k$ **disentangled** sub-features $\{z_i\}_{i=1}^k$ from $V$. The key component in this module is to maximize the distributional distance (such as the *KL divergence* and *Wasserstein distance*) between each pair of sub-features. We expect each sub-feature $z_i$ to encode exclusive aspects of the
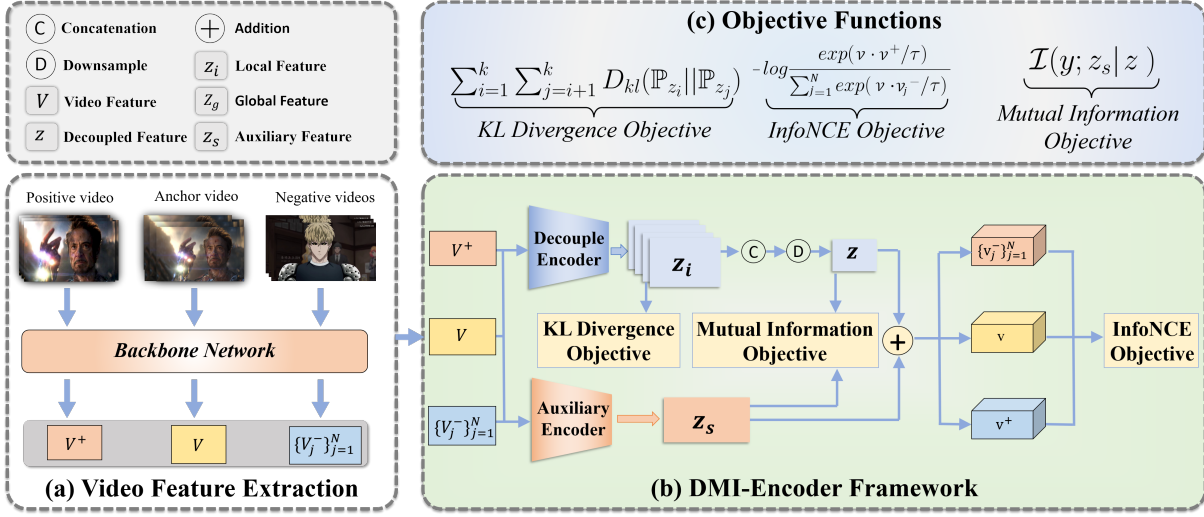
**Figure 2: Our pipeline: (1) In the training stage, the network input are an anchor video, a positive video (namely a video that is similar to the anchor video), and a set of negative videos (namely a set of videos that are dissimilar to the anchor video). We utilize MoCoV3 [5] backbone network to extract original features for the input videos. The original features go through a disentangled feature learning module and an auxiliary feature extraction module. The three objective functions shown in (c) constrain the network, mathematically guaranteeing the network to extract disentangled sub-features and the task-relevant auxiliary feature. (2) In the test stage, a query video is fed into the trained network to extract its features. Videos in the gallery are also input into the newtork to obtain their features. The cosine similarity between the query video and a video in the gallery is used to measure their similarity.**

original video feature. As such, we break the high dimensional feature into low dimensional disentangled components to remove redundancy and facilitate the extraction of task-relevant information. **(2)** In order to ensure the sufficiency of the feature representation, we further extract an auxiliary feature $\mathbf{z}_s$ to complete $\{\mathbf{z}_i\}_{i=1}^k$. In particular, we leverage a mutual information objective to effectuate task-relevant supplementary information extraction. The disentangled subfeatures $\{\mathbf{z}_i\}_{i=1}^k$ and the auxiliary feature $\mathbf{z}_s$ are then combined (concatenated) to arrive at our final feature representation. We would like to point out that the proposed approach has an edge in explicitly disentangling the feature, as well as in introducing mutual information supervision and sub-feature learning objectives.

In what follows, we will elaborate the key components of *disentangled sub-feature learning* and *auxiliary feature learning*, respectively.

## 3.2 Disentangled Sub-feature Learning Module

We can certainly train a direct end-to-end CNN network for extracting infringement-related video features, as is done in most previous methods [21, 23, 24]. However, such approaches implicitly mix different kinds of video features together, translating to high feature redundancy and low interpretability. Inspired by this, we believe it would be fruitful to investigate whether introducing supervision to disentangle the features would facilitate the task. With this goal in mind, we design a sub-features extraction module in the framework of contrastive learning and Kullback–Leibler divergence, which maps the original $d$-dimensional video feature to $k$ disentangled

lower dimensional sub-features. Contrastive learning supervises that similar videos have close embeddings and dissimilar videos have distinct embeddings, while Kullback–Leibler divergence enforces the $k$ sub-features to be different from each other.

Formally, we denote the $k$ extracted sub-features for a given anchor video $V$ as $\{\mathbf{z}_i\}_{i=1}^k$, and the concatenation of sub-features $\{\mathbf{z}_i\}_{i=1}^k$ as $\mathbf{v}$. For a positive video $V^+$ that is similar to $V$, we denote its concatenated sub-features as $\mathbf{v}^+$. Meanwhile, for a set of negative videos $\{V_j^-\}_{j=1}^N$ that are dissimilar to $V$, we denote their concatenated sub-features as $\{\mathbf{v}_1^-, \mathbf{v}_2^-, \cdots, \mathbf{v}_N^-\}$ respectively. We apply infoNCE loss [30] to $\mathbf{v}$, $\mathbf{v}^+$, and $\{\mathbf{v}_1^-, \mathbf{v}_2^-, \cdots, \mathbf{v}_N^-\}$, constraining that similar video pairs have similar embeddings while dissimilar pairs have distinct embeddings, which is given by:

$$\mathcal{L}_{\text{infoNCE}} = -log\frac{exp(\mathbf{v} \cdot \mathbf{v}^+/\tau)}{\sum_{j=1}^N exp(\mathbf{v} \cdot \mathbf{v}_j^-/\tau)}, \qquad (1)$$

where $\tau$ is a regulation parameter.

On top of the contrastive learning, we further add supervision on the extracted sub-features $\{\mathbf{z}_i\}_{i=1}^k$ of a video, ensuring that different sub-features encode minimally-overlapping aspects (semantics) of the original video. More specifically, for each two subfeatures $\mathbf{z}_i$ and $\mathbf{z}_j$ of a video, we try to maximize their difference, which is formulated as:

$$\max \ \mathcal{D}_{\text{KL}}(\mathbb{P}_{\mathbf{z}_i}||\mathbb{P}_{\mathbf{z}_j}) = \max \left[ -\int \mathbb{P}_{\mathbf{z}_i}(x) ln(\frac{\mathbb{P}_{\mathbf{z}_j}(x)}{\mathbb{P}_{\mathbf{z}_i}(x)})dx \right]. \quad (2)$$

Actually we have $k$ subfeatures for each video (namely $\frac{k*(k-1)}{2}$ subfeature pairs), therefore, the overall KL divergence objective is:

$$\max \sum_{i=1}^{k} \sum_{j=i+1}^{k} \mathcal{D}_{\text{KL}}(\mathbb{P}_{\mathbf{z}_i} || \mathbb{P}_{\mathbf{z}_j}) =$$

$$\max \left[ -\sum_{i=1}^{k} \sum_{j=i+1}^{k} \int \mathbb{P}_{\mathbf{z}_i}(x) ln(\frac{\mathbb{P}_{\mathbf{z}_j}(x)}{\mathbb{P}_{\mathbf{z}_i}(x)}) dx \right]. \tag{3}$$

Through such a principled disentangling of the original feature, we are able to remove redundancy and obtain compact disentangled sub-features, which also facilitate subsequent steps of task-relevant information extraction.

## 3.3 Auxiliary Feature Extraction Module

Up to this point, we are able to acquire the disentangled subfeatures $\{\mathbf{z}_i\}_{i=1}^{k}$ for a video. However, in the process of redundancy removing, the subfeatures might also miss some useful information in the original feature, leading to erosion of task-relevant information. Therefore, we propose to complete the subfeatures with an additional feature that consists of task-relevant information missed by subfeatures. To achieve this goal, we theoretically analyzed the mutual information between the label and the features, and derive a loss that maximizes the extraction of complementary task-relevant features. These allow us to enhance the extracted subfeatures and approach a better accuracy.

Formally, mutual information is a formal measure of the mutual dependency between random variables. The mutual information $\mathcal{I}(\mathbf{x}_1; \mathbf{x}_2)$ between two random variables $\mathbf{x}_1$ and $\mathbf{x}_2$ quantifies their correlated information and is defined as:

$$\mathcal{I}(\mathbf{x}_1; \mathbf{x}_2) = \mathbb{E}_{\mathbf{p}(\mathbf{x}_1, \mathbf{x}_2)} \left[ \log \frac{\mathbf{p}(\mathbf{x}_1, \mathbf{x}_2)}{\mathbf{p}(\mathbf{x}_1)\mathbf{p}(\mathbf{x}_2)} \right], \tag{4}$$

where $p(\mathbf{x}_1, \mathbf{x}_2)$ is the joint probability distribution of $\mathbf{x}_1$ and $\mathbf{x}_2$, and $p(\mathbf{x}_1)$ and $p(\mathbf{x}_2)$ are their marginals.

Technically, given the acquired subfeatures $\mathbf{z} = concatenate$ $\{\mathbf{z}_1, \mathbf{z}_2, \cdots, \mathbf{z}_k\}$, our primary objective is to maximize the amount of complementary task-relevant information in the auxiliary feature $\mathbf{z}_s$, which is given by:

$$\max \ \mathcal{I}(y; \mathbf{z}_s | \mathbf{z}), \tag{5}$$

where $y$ denotes the label (whether two videos are similar), and $\mathcal{I}(y; \mathbf{z}_s | \mathbf{z})$ represents the amount of task-relevant information in the auxiliary feature $\mathbf{z}_s$. Intuitively, maximizing this objective amounts to optimizing the additional task-relevant information we seek to extract from the original feature.

To simplify this problem, we factorize Eq. (5) as below:

$$\max \ \mathcal{I}(y; \mathbf{z}_s | \mathbf{z}) \Rightarrow \max \left[ \mathcal{I}(y; \mathbf{z}_s) \right.$$
$$\left. - \mathcal{I}(\mathbf{z}_s; \mathbf{z}) + \mathcal{I}(\mathbf{z}_s; \mathbf{z} | y) \right]. \tag{6}$$

Interestingly, $\mathcal{I}(\mathbf{z}_s; \mathbf{z} | y)$ represents the shared task-irrelevant information between $\mathbf{z}_s$ and $\mathbf{z}$. We may assume that the task-irrelevant information shared between $\mathbf{z}_s$ and $\mathbf{z}$ is negligible upon sufficient training [35]. This simplifies Eq. (6) to:

$$\max \ \mathcal{I}(y; \mathbf{z}_s | \mathbf{z}) \longrightarrow \max \left[ \mathcal{I}(y; \mathbf{z}_s) - \mathcal{I}(\mathbf{z}_s; \mathbf{z}) \right]. \tag{7}$$

To alleviate information dropping, we further introduce a regularization term:

$$\min \sum_{i=1}^{k} \mathcal{I}(y; \mathbf{z}_i | \mathbf{z}_s). \tag{8}$$

$\mathcal{I}(y; \mathbf{z}_i | \mathbf{z}_s)$ measures the vanishing task-relevant information in $\mathbf{z}_i$ during feature disentanglement. Analogous to the procedure from Eq. (6) to Eq. (7), we simplify the regularization term in Eq. (8) as follows:

$$\min \sum_{i=1}^{k} \mathcal{I}(y; \mathbf{z}_i | \mathbf{z}_s) \longrightarrow \min \sum_{i=1}^{k} [\mathcal{I}(y; \mathbf{z}_i) - \mathcal{I}(\mathbf{z}_i; \mathbf{z}_s)]. \tag{9}$$

The overall mutual information objective is:

$$\max \mathcal{I}(y; \mathbf{z}_s | \mathbf{z}) + \min \sum_{i=1}^{k} \mathcal{I}(y; \mathbf{z}_i | \mathbf{z}_s). \tag{10}$$

According to Eqs. (7), (9), and (10), the mutual information loss can be finally formulated into:

$$\mathcal{L}_{MI} = -[\mathcal{I}(y; \mathbf{z}_s) - \mathcal{I}(\mathbf{z}_s; \mathbf{z})] + \sum_{i=1}^{k} [\mathcal{I}(y; \mathbf{z}_i) - \mathcal{I}(\mathbf{z}_i; \mathbf{z}_s)]. \tag{11}$$

**Training Objective**. We would like to point out that the overall training objective for our end-to-end network consists of two parts. **(1)** Contrastive learning loss $\mathcal{L}_{\text{infoNCE}}$ and KL divergence loss that supervise the extraction of disentangled sub-features, which is given by:

$$\mathcal{L}_{\text{decouple}} = \mathcal{L}_{\text{infoNCE}}$$
$$- \alpha \cdot \left[ -\sum_{i=1}^{k} \sum_{j=i+1}^{k} \int \mathbb{P}_{\mathbf{z}_i}(x) ln(\frac{\mathbb{P}_{\mathbf{z}_j}(x)}{\mathbb{P}_{\mathbf{z}_i}(x)}) dx \right]. \tag{12}$$

**(2)** The mutual information loss $\mathcal{L}_{MI}$, which is presented in Eq. (11), constrains the extraction of the auxiliary feature. As such, the overall loss function is:

$$\mathcal{L}_{\text{total}} = \mathcal{L}_{\text{decouple}} + \mathcal{L}_{\text{MI}}. \tag{13}$$

## 4 EXPERIMENTS

In this section, we evaluate the proposed approach on two large-scale benchmark datasets, SVD and VCSL. We seek to answer the following research questions.

- RQ1: How is the proposed method comparing to state-of-the-art approaches?
- RQ2: How much do different components of our method contribute to its performance?
- RQ3: What interesting insights and findings can we obtain from the empirical results?

Next, we first present the experimental settings, followed by answering the research questions one by one.
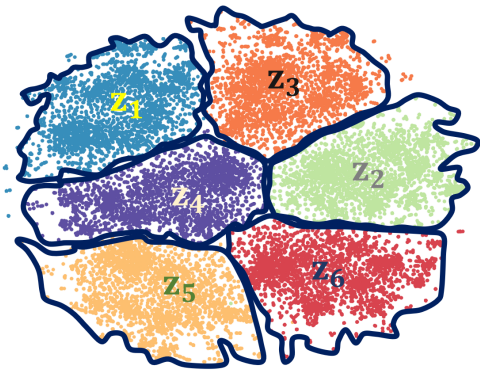
**Figure 3: We visualize the features of 6,157 randomly selected videos. $z_i$ denotes the $i^{th}$ sub-feature, which has 256 dimensions. We use TSNE to reduce the dimension of $z_i$ to 2.**

## 4.1 Experimental Settings

**Datasets** The **SVD** [16] dataset is a large-scale benchmark dataset for infringing video retrieval. The dataset contains over 500,000 videos and over 30,000 labeled pairs of infringing (similar) videos. The categories of videos are almost all-encompassing, including movies, TV series, commentary videos, daily videos, *etc.* The **VCSL** [13] dataset consists of more than 167,000 video infringement pairs with diverse video categories and varying video durations.

**Implementation Details** Our DMI (feature <u>D</u>isentanglement and <u>M</u>utual <u>I</u>nformation maximization) framework is implemented with PyTorch 1.4.0. For pre-processing, we divide the videos into frames and feed them into pre-trained network MoCoV3 [5] to extract the original feature for each frame. In the training process, the unlabeled videos are deemed as dissimilar to other videos and serve as negative training samples for an anchor video, which increases the number of training samples and improves the robustness of our model. Training is done with 4 Nvidia Geforce RTX 2080 Ti GPUs. The batch sizes on SVD and VCSL datasets are set to 64 and 16, respectively. In contrastive learning, the ratio of positive samples to negative samples for an anchor video is 64:2048. All training processes are terminated within 300 epochs. The number of sub-features is set to $k = 6$. For evaluation, the widely used top-100 mAP [16] and F-score [13] metrics are adopted.

## 4.2 Comparisons with State-of-the-art Methods (RQ1)

First, we benchmark our approach against state-of-the-art methods on the **SVD dataset**. The performance of different methods are presented in terms of Top-100 mAP in Table 1. A total of 8 methods are compared, including DML [21], CNN-L [20], CNN-V [20], IsoH [18], ITQ [9], HDML [29], SVRTN [14], and ours. Specifically, 1) DML proposes to early or late fuse frame-level features into a single video vector, which is then fine-tuned by deep metric learning. 2) CNN-L & CNN-V [20] advocate to convert intermediate CNN features into one vector via layer and vector aggregation schemes, respectively. 3) SVRTN [14] exploits a transformer structure to aggregate frame-level features into clip-level features and learns

**Table 1: Comparison with existing methods on the SVD dataset.**

| Method | Top-100 mAP | Method | Top-100 mAP |
|---|---|---|---|
| ITQ [9] | 0.301 | CNN-V [20] | 0.251 |
| IsoH [18] | 0.309 | DML [21] | 0.813 |
| HDML [29] | 0.316 | SVRTN [14] | 0.871 |
| CNN-L [20] | 0.610 | **Our Method** | **0.901** |

**Table 2: Comparison with existing methods on the VCSL dataset.**

| Method | F-score | Method | F-score |
|---|---|---|---|
| ViT [8] | 57.61 | R-MAC [38] | 58.75 |
| DINO [3] | 59.99 | ISC [43] | 61.36 |
| VGG [31] | 51.28 | ViSiL [19] | 61.46 |
| Resnet [12] | 52.07 | **Our method** | **61.69** |

the discriminative information from the interactions among clip frames. 4) ITQ [9] learns similarity-preserving binary codes for image retrieval by proposing an alternating minimization scheme that minimizes the quantization error. 5) IsoH [18] improves ITQ and presents isotropic hashing strategy to learn projection functions that produce projected dimensions with isotropic variances. 6) HDML [29] develops a new loss-augmented inference algorithm that overcomes discontinuous optimization of the mapping from data to binary codes. From Table 1, we observe that metric learning-based and transformer-based approaches, namely DML and SVRTN, achieve the current state-of-the-art performance. Conventional methods [9, 18, 29], which try to map a frame into binary codes, are surpassed by deep learning methods. Our method is able to outperform DML and SVRTN with a 8.8% and 3.0% mAP gain, and overall achieves a 90.1% TOP-100 mAP. These empirical evidences suggest the feasibility of the proposed approach.

Further, we also conduct evaluations on the **VCSL dataset**. The comparison results are illustrated in Table 2. Specifically, to evaluate the methods, we follow the F-score metric proposed by the VCSL dataset [13], which serves as the official comparison metric of the dataset and measures the overlapped similar clips between two videos. Following [13], we choose the Temporal Network (TN) [34] as our alignment method. We compare our method with the approaches that achieve the current state-of-the-art performance on the VCSL dataset, including ViT [8], DINO [3], R-MAC [38], ViSiL [19], and ISC [43]. Two baselines VGG [31] and Resnet [12] are also included in the comparison. For VGG [31], we use the VGG [31] network to extract the frame features and employ cosine similarity to compute the distance between frames. For Resnet [12], we use the Resnet-50 [12] network to extract frame features and adopt cosine similarity to compute the distance between frames. From the table, we have the following observations. Due to the inherent challenge in precisely identifying overlapped similar clips between two videos, existing methods have yet achieved impressive F-score on this large dataset. In particular, the current state-of-the-art methods ViSiL [19] and ISC [43] obtain 61.36% and 61.46% F-score respectively on

| Features | MoCoV3 | | VGG | |
|---|---|---|---|---|
| | Top-100 mAP | Top-inf mAP | Top-100 mAP | Top-inf mAP |
| Sub-feature $z_1$ | 0.863 | 0.857 | 0.826 | 0.805 |
| Sub-feature $z_2$ | 0.861 | 0.855 | 0.825 | 0.801 |
| Sub-feature $z_3$ | 0.862 | 0.849 | 0.795 | 0.778 |
| Sub-feature $z_4$ | 0.867 | 0.843 | 0.801 | 0.790 |
| Sub-feature $z_5$ | 0.863 | 0.847 | 0.824 | 0.807 |
| Sub-feature $z_6$ | 0.851 | 0.839 | 0.821 | 0.801 |
| Global feature | **0.901** | **0.887** | **0.838** | **0.813** |

Table 3: Ablation study on sub-features.

Table 4: Ablation of different components in our method.

| Method | Disentangle Module | Auxiliary Module | Disentangle Loss | Mi Loss | Top-100 mAP | Top-inf mAP |
|---|---|---|---|---|---|---|
| (a) | Remove | | | | 0.873 | 0.856 |
| (b) | | Remove | | | 0.881 | 0.862 |
| (c) | | | Remove | | 0.876 | 0.858 |
| (d) | | | | Remove | 0.883 | 0.861 |
| Default | | | | | **0.901** | **0.887** |

Table 5: The impact of varying the number of sub-features.

| Feature count | top-100 mAP | top-inf mAP |
|---|---|---|
| 2 | 88.43% | 87.09% |
| 4 | 88.47% | 86.82% |
| 6 | **90.12%** | **88.70%** |
| 8 | 88.87% | 87.56% |

this dataset. Our method consistently achieves the state-of-the-art performance.

## 4.3 Ablation Study (RQ2)

**Effect of the *disentangled sub-feature learning* module and the *auxiliary feature extraction* module.** By default, the proposed *disentangled sub-feature learning* module and the *auxiliary feature extraction* module are coupled together to approach high performance. We are interested in studying the impact of removing each module respectively from the proposed method.

Towards this aim, we empirically study the impact of removing the two modules from the framework. **(a)** For the fisrt setting, we remove the sub-feature learning module in our framework, and only use the auxiliary feature extraction module to extract features. **(b)** For the second setting, we remove the global feature extraction module in our framework, and only adopt the sub-features extraction module to learn representations.

The two modules are shown in Fig. 4. When the sub-feature learning module is removed, we only compute the *infoNCE* and the *mutual information* objectives, where *infoNCE* objective guarantees that two similar videos get similar features while the *mutual information* objective enforces to extract the auxiliary feature.

We compare them with the default network. Experimental results on the SVD dataset is demonstrated in Table 4 , where both top-100 mAP and top-inf mAP results are reported. We see that without the sub-features extraction module, the proposed method undergoes
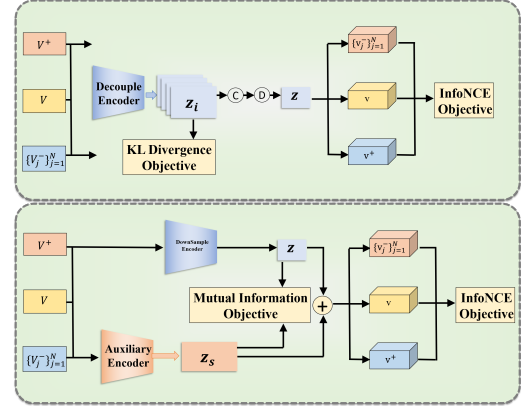


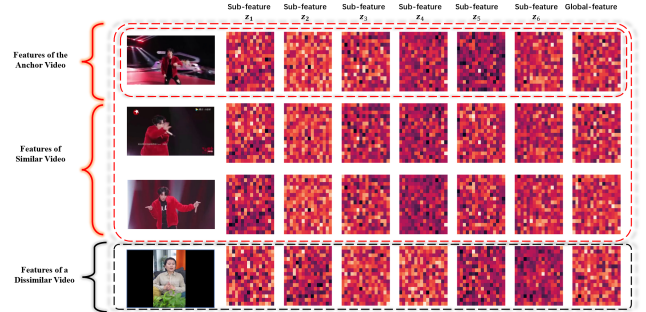Figure 4: The architectures of the two ablation modules.



Figure 5: Features visualization for similar and dissimilar videos.

2.8% top-100 mAP and 3.1% top-inf mAP drops, respectively. These empirical evidences indicate the importance of the sub-features extraction module, which contributes in removing redundancy and disentangling features. Meanwhile, without the auxiliary feature extraction module, the method undergoes 2.0% top-100 mAP and 2.5% top-inf mAP drops, respectively. This suggests the significance of the auxiliary feature extraction module, which contributes in capturing more complete task-relevant information. Removing the sub-features extraction module leads to higher performance drop than removing the auxiliary feature extraction module.

**Effect of the disengtangle loss and mutual information loss.** Furthermore, we study the impact of removing the proposed

disengtangle loss and mutual information loss from our network. More specifically, we remove the disengtangle loss and mutul information loss respectively from the network while preserving all other components. As demonstrated in **(c)** and **(d)** in Table 4, the top-100 mAP and top-inf mAP drop 2.5% and 2.9% respectively when the disengtangle loss is removed, while top-100 mAP and top-inf mAP drop 1.8% and 2.6% respectively when the mutual information loss is removed. This indicates that the disengtangle loss and mutual information loss both contribute to performance gain.

**Number of sub-features.** By default, in our method the number of sub-features is set to 6. It is interesting to see the effect of enlarging or reducing the number of sub-features. We illustrate the emprical results in Table 5. We observe that enlarging the number of sub-laysers tends to gradualy increase the accuracy. The highest accuracy is obtained when the number of features is set to 6.

## 4.4 Insights (RQ3)

We make some key findings in our research. Firstly, we find that in cases of video infringement, the videos are often modified by cropping, blocking parts of the picture, splicing, and editing content. To extract the original frame features, we test the VGG and MoCoV3 (Resnet) networks as backbone networks. Our experiments showed that the MoCoV3 feature outperformed the VGG feature in terms of accuracy. We attribute this to the fact that the MoCoV3 network inherently considers data augmentations, which are commonly used in video infringement, *e.g.*, cropping, grayscale, blocking parts of the picture, and horizontal flipping.

Secondly, we empirically study the separability of the extracted sub-features. To investigate this, we randomly select 6,157 videos and visualized their extracted sub-features using TSNE. The results are shown in Figure 3. We set $k$ to 6, so six sub-features $\{z_i\}_{i=1}^6$ are depicted. The dimension of $z_i$ is 256. We conduct dimension reduction using TSNE. Interestingly, we find that the sub-features are disentangled from each other.

Furthermore, we visualize the features of similar and dissimilar videos in Fig. 5. We find that sub-features for similar videos are similar to each other, while dissimilar videos have quite different sub-features. Moreover, the sub-features for the same video are distinct from each other, which reconfirms the separability of the extracted sub-features.

We randomly sample 978 similar video pairs. We divide the 978 pairs of videos into two sets $A$ and $B$, where the two similar videos in each pair are put into two different sets. We compute the similarity matrix between the two sets of videos by utilizing the proposed method. The similarity matrix is visualized in Figure 6**(a)**, where the $x$-axis represents the 978 videos of set $A$ and $y$-axis denotes the 978 videos of set $B$. The color of a pixel $(i, j)$ reflects the similarity between the $i^{th}$ video of set $A$ and the $j^{th}$ video of set $B$. Figure 6**(b)** shows the ground-truth similarity matrix. From Figure 6**(a)** and Figure 6 **(b)**, we observe that the results of our method is very close to the ground truth. Further, we zoom in the similarity matrix in Figure 6**(a)** by sampling 10 pairs of videos from the matrix. The sampled sub-matrix is demonstrated in Figure 7**(a)**. Figure 7**(a)** shows clearer details of the similarity matrix while Figure 7**(b)** provides the corresponding ground truth. We see that the results of our method are in consistent with the ground truth.
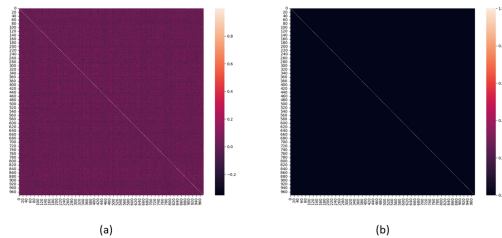


**Figure 6: (a): The similarity matrix computed by our method. Experiments are conducted on the SVD dataset. (b): The corresponding ground-truth similarity matrix of (a).**
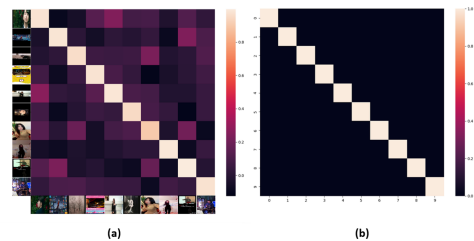


**Figure 7: (a): The sub-matrix sampled from the computed similarity matrix. (b): The corresponding ground-truth similarity matrix of (a).**

During the experiments, another interesting phenomena catches our attention. We are curious to know the effect of using each extracted sub-feature alone in detecting infringements. Towards this aim, we conduct experiments by using each sub-feature alone for computing video similarity. As shown Table 3, we found that using only one extracted sub-feature also yields good result. However, utilizing all the sub-features and the auxiliary feature achieves better performance.

## 5 CONCLUSION

In this work, we have proposed a novel framework for infringing video retrieval, which is equipped with feature disentanglement and mutual information maximization. Within the framework, we combine contrastive learning and the KL divergence maximization to effectively supervise the disentangling of subfeatures. Further, we theoretically derive a mutual information objective for supervising the extraction of auxiliary and task-relevant features that might be missed by sub-features. Extensive experiments demonstrate that our method achieves state-of-the-art results on large-scale benchmark datasets, SVD and VCSL.

# REFERENCES

[1] Lorenzo Baraldi, Matthijs Douze, Rita Cucchiara, and Hervé Jégou. 2018. LAMV: Learning to align and match videos with kernelized temporal layers. In *Proceedings of the IEEE conference on computer vision and pattern recognition*. 7804–7813.

[2] Yang Cai, Linjun Yang, Wei Ping, Fei Wang, Tao Mei, Xian-Sheng Hua, and Shipeng Li. 2011. Million-scale near-duplicate video retrieval system. In *Proceedings of the 19th ACM international conference on Multimedia*. 837–838.

[3] Mathilde Caron, Hugo Touvron, Ishan Misra, Hervé Jégou, Julien Mairal, Piotr Bojanowski, and Armand Joulin. 2021. Emerging Properties in Self-Supervised Vision Transformers. *CoRR* abs/2104.14294 (2021). arXiv:2104.14294 https://arxiv.org/abs/2104.14294

[4] Ting Chen, Simon Kornblith, Mohammad Norouzi, and Geoffrey Hinton. 2020. A simple framework for contrastive learning of visual representations. In *International conference on machine learning*. PMLR, 1597–1607.

[5] Xinlei Chen*, Saining Xie*, and Kaiming He. 2021. An Empirical Study of Training Self-Supervised Vision Transformers. *arXiv preprint arXiv:2104.02057* (2021).

[6] Xun Deng, Wenjie Wang, Fuli Feng, Hanwang Zhang, Xiangnan He, and Yong Liao. 2023. Counterfactual Active Learning for Out-of-Distribution Generalization. In *Proceedings of the 61st Annual Meeting of the Association for Computational Linguistics (Volume 1: Long Papers)*. 11362–11377.

[7] Jianfeng Dong, Xirong Li, and Cees GM Snoek. 2018. Predicting visual features from text for image and video caption retrieval. *IEEE Transactions on Multimedia* 20, 12 (2018), 3377–3388.

[8] Alexey Dosovitskiy, Lucas Beyer, Alexander Kolesnikov, Dirk Weissenborn, Xiaohua Zhai, Thomas Unterthiner, Mostafa Dehghani, Matthias Minderer, Georg Heigold, Sylvain Gelly, Jakob Uszkoreit, and Neil Houlsby. 2020. An Image is Worth 16x16 Words: Transformers for Image Recognition at Scale. *CoRR* abs/2010.11929 (2020). arXiv:2010.11929 https://arxiv.org/abs/2010.11929

[9] Yunchao Gong, Svetlana Lazebnik, Albert Gordo, and Florent Perronnin. 2012. Iterative quantization: A procrustean approach to learning binary codes for large-scale image retrieval. *IEEE transactions on pattern analysis and machine intelligence* 35, 12 (2012), 2916–2929.

[10] Yanbin Hao, Shuo Wang, Pei Cao, Xinjian Gao, Tong Xu, Jinmeng Wu, and Xiangnan He. 2022. Attention in attention: Modeling context correlation for efficient video classification. *IEEE Transactions on Circuits and Systems for Video Technology* 32, 10 (2022), 7120–7132.

[11] Kaiming He, Haoqi Fan, Yuxin Wu, Saining Xie, and Ross Girshick. 2020. Momentum contrast for unsupervised visual representation learning. In *Proceedings of the IEEE/CVF conference on computer vision and pattern recognition*. 9729–9738.

[12] Kaiming He, Xiangyu Zhang, Shaoqing Ren, and Jian Sun. 2015. Deep Residual Learning for Image Recognition. *CoRR* abs/1512.03385 (2015). arXiv:1512.03385 http://arxiv.org/abs/1512.03385

[13] Sifeng He, Xudong Yang, Chen Jiang, et al. 2022. A Large-scale Comprehensive Dataset and Copy-overlap Aware Evaluation Protocol for Segment-level Video Copy Detection. In *Proceedings of the IEEE/CVF Conference on Computer Vision and Pattern Recognition*. 21086–21095.

[14] Xiangteng He, Yulin Pan, Mingqian Tang, and Yiliang Lv. 2021. Self-supervised Video Retrieval Transformer Network. *CoRR* abs/2104.07993 (2021). arXiv:2104.07993 https://arxiv.org/abs/2104.07993

[15] Yaocong Hu and Xiaobo Lu. 2018. Learning spatial-temporal features for video copy detection by the combination of CNN and RNN. *Journal of Visual Communication and Image Representation* 55 (2018), 21–29.

[16] Qing-Yuan Jiang, Yi He, Gen Li, Jian Lin, Lei Li, and Wu-Jun Li. 2019. SVD: A large-scale short video dataset for near-duplicate video retrieval. In *Proceedings of the IEEE/CVF International Conference on Computer Vision*. 5281–5289.

[17] H. Jing, S. R. Kumar, M. Mitra, W. J. Zhu, and R. Zabih. 1999. Spatial Color Indexing and Applications. *International Journal of Computer Vision* 35, 3 (1999), 245–268.

[18] W. Kong and W. J. Li. 2012. Isotropic Hashing. *Advances in neural information processing systems* 2 (2012), 1646–1654.

[19] Giorgos Kordopatis-Zilos, Symeon Papadopoulos, Ioannis Patras, and Ioannis Kompatsiaris. 2019. ViSiL: Fine-grained Spatio-Temporal Video Similarity Learning. *CoRR* abs/1908.07410 (2019). arXiv:1908.07410 http://arxiv.org/abs/1908.07410

[20] Giorgos Kordopatis-Zilos, Symeon Papadopoulos, Ioannis Patras, and Yiannis Kompatsiaris. 2017. Near-duplicate video retrieval by aggregating intermediate cnn layers. In *International conference on multimedia modeling*. Springer, 251–263.

[21] Giorgos Kordopatis-Zilos, Symeon Papadopoulos, Ioannis Patras, and Yiannis Kompatsiaris. 2017. Near-duplicate video retrieval with deep metric learning. In *Proceedings of the IEEE international conference on computer vision workshops*. 347–356.

[22] Kaiyang Liao, Hao Lei, Yuanlin Zheng, Guangfeng Lin, Congjun Cao, Mingzhu Zhang, and Jie Ding. 2018. IR feature embedded bof indexing method for near-duplicate video retrieval. *IEEE Transactions on Circuits and Systems for Video Technology* 29, 12 (2018), 3743–3753.

[23] Hao Liu, Qingjie Zhao, Hao Wang, Peng Lv, and Yanming Chen. 2017. An image-based near-duplicate video retrieval and localization using improved edit distance. *Multimedia Tools and Applications* 76, 22 (2017), 24435–24456.

[24] Jiajun Liu, Zi Huang, Hongyun Cai, Heng Tao Shen, Chong Wah Ngo, and Wei Wang. 2013. Near-duplicate video retrieval: Current research and future trends. *ACM Computing Surveys (CSUR)* 45, 4 (2013), 1–23.

[25] Zhenguang Liu, Haoming Chen, Runyang Feng, Shuang Wu, Shouling Ji, Bailin Yang, and Xun Wang. 2021. Deep Dual Consecutive Network for Human Pose Estimation. In *CVPR*. 525–534. https://doi.org/10.1109/CVPR46437.2021.00059

[26] Zhenguang Liu, Runyang Feng, Haoming Chen, Shuang Wu, Yixing Gao, Yunjun Gao, and Xiang Wang. 2022. Temporal Feature Alignment and Mutual Information Maximization for Video-Based Human Pose Estimation. In *Proceedings of the IEEE/CVF Conference on Computer Vision and Pattern Recognition*. 11006–11016.

[27] Zhenguang Liu, Shuang Wu, Shuyuan Jin, Qi Liu, Shijian Lu, Roger Zimmermann, and Li Cheng. 2019. Towards Natural and Accurate Future Motion Prediction of Humans and Animals. In *CVPR*. 10004–10012. https://doi.org/10.1109/CVPR.2019.01024

[28] Zhenguang Liu, Sifan Wu, Chejian Xu, Xiang Wang, Lei Zhu, Shuang Wu, and Fuli Feng. 2022. Copy Motion From One to Another: Fake Motion Video Generation. In *IJCAI*. 1223–1231. https://doi.org/10.24963/ijcai.2022/171

[29] Mohammad Norouzi, David J Fleet, and Russ R Salakhutdinov. 2012. Hamming distance metric learning. *Advances in neural information processing systems* 25 (2012).

[30] Aaron van den Oord, Yazhe Li, and Oriol Vinyals. 2018. Representation learning with contrastive predictive coding. *arXiv preprint arXiv:1807.03748* (2018).

[31] Karen Simonyan and Andrew Zisserman. 2014. Very deep convolutional networks for large-scale image recognition. *arXiv preprint arXiv:1409.1556* (2014).

[32] J. Song, Y. Yang, Z. Huang, H. T. Shen, and R. Hong. 2011. Multiple feature hashing for real-time large scale near-duplicate video retrieval. In *International Conference on Multimedea*. 423.

[33] Jingkuan Song, Yi Yang, Zi Huang, Heng Tao Shen, and Jiebo Luo. 2013. Effective multiple feature hashing for large-scale near-duplicate video retrieval. *IEEE Transactions on Multimedia* 15, 8 (2013), 1997–2008.

[34] Hung-Khoon Tan, Chong-Wah Ngo, Richard Hong, and Tat-Seng Chua. 2009. Scalable detection of partial near-duplicate videos by visual-temporal consistency. In *Proceedings of the 17th ACM international conference on Multimedia*. 145–154.

[35] Xudong Tian, Zhizhong Zhang, Shaohui Lin, Yanyun Qu, Yuan Xie, and Lizhuang Ma. 2021. Farewell to mutual information: Variational distillation for cross-modal person re-identification. In *Proceedings of the IEEE/CVF Conference on Computer Vision and Pattern Recognition*. 1522–1531.

[36] Naftali Tishby, Fernando C Pereira, and William Bialek. 2000. The information bottleneck method. *arXiv preprint physics/0004057* (2000).

[37] Naftali Tishby and Noga Zaslavsky. 2015. Deep learning and the information bottleneck principle. In *2015 ieee information theory workshop (itw)*. IEEE, 1–5.

[38] Giorgos Tolias, Ronan Sicre, and Hervé Jégou. 2016. Particular object retrieval with integral max-pooling of CNN activations. In *4th International Conference on Learning Representations, ICLR 2016, San Juan, Puerto Rico, May 2-4, 2016, Conference Track Proceedings*, Yoshua Bengio and Yann LeCun (Eds.). http://arxiv.org/abs/1511.05879

[39] Xun Yang, Jianfeng Dong, Yixin Cao, Xun Wang, Meng Wang, and Tat-Seng Chua. 2020. Tree-augmented cross-modal encoding for complex-query video retrieval. In *Proceedings of the 43rd international ACM SIGIR conference on research and development in information retrieval*. 1339–1348.

[40] Xun Yang, Shanshan Wang, Jian Dong, Jianfeng Dong, Meng Wang, and Tat-Seng Chua. 2022. Video moment retrieval with cross-modal neural architecture search. *IEEE Transactions on Image Processing* 31 (2022), 1204–1216.

[41] Yuheng Yang, Haipeng Chen, Zhenguang Liu, Yingda Lyu, Beibei Zhang, Shuang Wu, Zhibo Wang, and Kui Ren. 2023. Action Recognition with Multi-stream Motion Modeling and Mutual Information Maximization. *CoRR* abs/2306.07576 (2023). https://doi.org/10.48550/arXiv.2306.07576

[42] Yifang Yin, Harsh Shrivastava, Ying Zhang, Zhenguang Liu, Rajiv Ratn Shah, and Roger Zimmermann. 2021. Enhanced audio tagging via multi-to single-modal teacher-student mutual learning. In *Proceedings of the AAAI conference on artificial intelligence*. 10709–10717.

[43] Shuhei Yokoo. 2021. Contrastive Learning with Large Memory Bank and Negative Embedding Subtraction for Accurate Copy Detection. *CoRR* abs/2112.04323 (2021). arXiv:2112.04323 https://arxiv.org/abs/2112.04323

[44] Jing Zhang, Deng-Ping Fan, Yuchao Dai, Xin Yu, Yiran Zhong, Nick Barnes, and Ling Shao. 2021. RGB-D saliency detection via cascaded mutual information minimization. In *Proceedings of the IEEE/CVF International Conference on Computer Vision*. 4338–4347.